

DiskGNN: Bridging I/O Efficiency and Model Accuracy for Out-of-Core GNN Training

Renjie Liu^{1,4,*}, Yichuan Wang^{2,*}, Xiao Yan³, Zhenkun Cai⁴, Minjie Wang⁴, Haitian Jiang⁵
Bo Tang¹, Jinyang Li⁵

¹Southern University of Science and Technology ²Shanghai Jiao Tong University

³Centre for Perceptual and Interactive Intelligence ⁴AWS Shanghai AI Lab ⁵New York University

ABSTRACT

Graph neural networks (GNNs) are machine learning models specialized for graph data and widely used in many applications. To train GNNs on large graphs that exceed CPU memory, several systems store data on disk and conduct out-of-core processing. However, these systems suffer from either *read amplification* when reading node features that are usually smaller than a disk page or *degraded model accuracy* by treating the graph as disconnected partitions. To close this gap, we build a system called *DiskGNN*, which achieves high I/O efficiency and thus fast training without hurting model accuracy. The key technique used by DiskGNN is *offline sampling*, which helps decouple *graph sampling* from *model computation*. In particular, by conducting graph sampling beforehand, DiskGNN acquires the node features that will be accessed by model computation, and such information is utilized to pack the target node features contiguously on disk to avoid read amplification. Besides, DiskGNN also adopts designs including *four-level feature store* to fully utilize the memory hierarchy to cache node features and reduce disk access, *batched packing* to accelerate the feature packing process, and *pipelined training* to overlap disk access with other operations. We compare DiskGNN with Ginex and MariusGNN, which are state-of-the-art systems for out-of-core GNN training. The results show that DiskGNN can speed up the baselines by over 8x while matching their best model accuracy.

1 INTRODUCTION

Graph data is ubiquitous in domains such as e-commerce [1], finance [2, 3], bio-informatics [4], and social networks [5]. As machine learning models specialized for graph data, graph neural networks (GNNs) achieve high accuracy for various graph tasks (e.g., node classification [6], link prediction [7], and graph clustering [8]) and hence are used in many applications like recommendation [9], fraud detection [10], and pharmacy [11]. In particular, GNNs compute an embedding for each node v in the graph by recursively aggregating the input features of v 's neighbors. For large graphs, to reduce the cost of aggregating all neighbors, *graph sampling* is usually adopted to sample some of the neighbors for aggregation.

Large graphs with millions of nodes and billions of edges are common in practice [12–14]. They may not fit in the main memory of a single machine and require solutions to scale up GNN training. Some systems (e.g., DistDGL [15], DSP [16], and P3 [17]) conduct distributed training across multiple machines, by partitioning the graph data and training computation over the machines. However, distributed solutions are expensive to deploy and suffer

Table 1: Execution statistics of two disk-based GNN training systems and our DiskGNN on the Ogbn-papers100M graph. The CPU memory is set as 10% of the dataset size.

Metrics	Ginex [18]	MariusGNN [20]	DiskGNN (ours)
Avg. epoch time (sec)	580	165	76.3
Disk access time (sec)	412	27.1	51.2
Disk access volume (GB)	484	6.46	73.9
Test accuracy (%)	65.9	64.0	65.9

from low GPU utilization due to the heavy inter-machine communication required to handle the cross-partition edges. Observing that solid-state disks (SSDs) are now cheap, capacious, and reasonably fast (with a bandwidth of 2-7GB/s), some systems (e.g., Ginex [18], GIDS [19], MariusGNN [20], and Helios [21]) conduct out-of-core training by storing the graph data on the disk of a single machine. Compared with distributed systems, these disk-based solutions are more accessible and cost effective.

Existing disk-based systems and their limitations. Most existing disk-based systems, including Ginex [18], GIDS [19] and Helios [21], adopt the same workflow as in-memory training systems. Specifically, for each mini-batch training step, they first perform graph sampling to determine which node features are needed, fetch those features, and then perform the batch's model computation; the difference is that on-disk systems read node features from the disk instead of CPU memory. Despite various system optimizations, such as CPU memory caching [18] and concurrent disk reads [19, 21], a fundamental problem with these systems lies in their random small reads pattern, whereby only a single node's feature (typically < 512 bytes) is used for each disk read at 4KB page granularity, causing substantial *read amplification* and poor I/O efficiency. As shown in Table 1, Ginex spends most of its training time on disk access, and its disk read volume (484GB) is much larger than the total amount of sampled node features (73.9GB, as achieved by our system DiskGNN) under the same cache size constraint.

To avoid read amplification, MariusGNN [20] pre-processes the graph to enable more efficient large reads during training. Specifically, MariusGNN stores the graph in a set of partitions on disk and swaps in a few of them to CPU memory during each training epoch. Sampling of mini-batches is done on the sub-graph from all memory-resident partitions. Although MariusGNN achieves efficient disk I/O, its mini-batch sampling is quite biased as it ignores

*Renjie and Yichuan contribute equally.

nodes from any non-memory-resident partition, thereby resulting in degraded model accuracy as shown in Table 1.

Our system DiskGNN. To eliminate the aforementioned tension between I/O efficiency and model accuracy, we build a new out-of-core GNN system (DiskGNN) based on an alternative training paradigm called *offline sampling*. With offline sampling, DiskGNN decouples the two main stages of GNN training, i.e., graph sampling and model training, and conducts graph sampling for many mini-batches before model computation. In this way, offline sampling can determine the node features that will be accessed during model computation and use the information to optimize the data layout proactively for efficient access. Specifically, we group the node features according to their access frequencies and assign them to a *four-level feature store* that involves GPU memory, CPU memory, and disk, with the principle of caching more popular node features in faster storage. More importantly, to avoid read amplification, we pre-process the node features that each mini-batch needs to read from disk by packing them into a consecutive disk region. As naive packing may result in very large storage overhead, we trade off between I/O efficiency and disk space with a hybrid packing strategy, which consists of shared features among mini-batches that use *node reordering* to reduce read amplification and dedicated features for each mini-batch that use *consecutive packing*. We also make the pre-processing and packing efficient using *batched packing*, which sequentially reads large chunks of node features and writes back the required node features for all mini-batches in one pass. Besides out-of-core training, we also discuss the potential benefits of offline sampling for other scenarios.

We implement DiskGNN on top of the Deep Graph Library (DGL) [22], one of the most popular open-source frameworks for deep learning on graphs. DiskGNN adopts a training pipeline to overlap the disk access of a mini-batch with the model computation of the previous mini-batches. We also carefully implement the I/O operations of DiskGNN for efficiency and provide simple APIs for usability.

We evaluate DiskGNN on 4 large public graph datasets and 2 predominate GNN model architectures. The results show that DiskGNN consistently yields shorter training time than both Ginex and MarisGNN with an average speedup of 7.5x and 2.5x over the two of them, respectively. Moreover, DiskGNN matches the model accuracy of Ginex while being significantly more accurate than MarisGNN. We also conduct micro experiments to validate the effectiveness of our designs. The results show that the batched read-write can accelerate pre-processing by 7.3x, and the training pipeline can speed up training by over 2x.

To summarize, make the following contributions in this paper.

- We observe that existing disk-based GNN training systems face the tension between I/O efficiency and model accuracy and that they cannot achieve both simultaneously.
- We design DiskGNN to achieve both I/O efficiency and model accuracy by exploiting offline sampling, which collects the data access beforehand to optimize the data layout for access.
- We propose a suite of designs tailored for on-disk workloads to make DiskGNN efficient, which include four-level feature store, batched feature packing, and pipelined training.

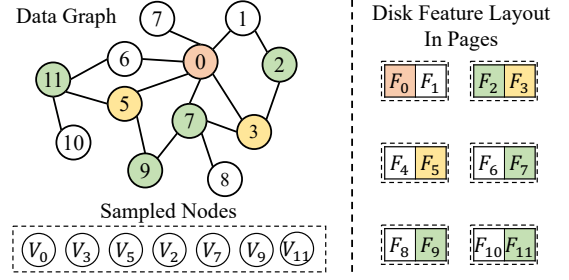


Figure 1: An illustration for node-wise graph sampling. The seed node is v_0 , and the sampled 1-hop and 2-hop neighbors are marked in yellow and green, respectively. We assume that two node features take up a disk page.

2 BACKGROUND ON GNN TRAINING

GNN basics. GNN models usually take a data graph $G = (V, E)$, where V and E are the node set and edge set, and each node $v \in V$ comes with a feature vector h_v^0 that describes its properties. For instance, in the Ogbn-papers100M dataset, each node is a paper, an edge indicates that one paper cites another paper, and each node feature vector is a 128-dimension float embedding of a paper’s title and abstract. A GNN model typically stacks multiple graph aggregation layers with each layer aggregating the embeddings of a node’s neighbors to compute an embedding for the node. Specifically, in the k^{th} layer, the output embedding h_v^k of node v is computed as

$$h_v^k = \sigma[W^k \cdot \text{AGG}_k(\{h_u^{k-1}, \forall u \in \mathcal{N}(v)\})], \quad (1)$$

where set $\mathcal{N}(v)$ contains the neighbors of node v in the graph, and h_u^{k-1} is the embedding of node u in the $(k-1)^{\text{th}}$ layer. For the first layer, h_u^0 is the input node feature vector. $\text{AGG}_k(\cdot)$ is the neighbor aggregation function, and typical choices include mean, max, sum, and concatenate. W^k is a projection matrix of size $d' \times d$, where d' is the dimension of h_v^k and d is the dimension of h_u^{k-1} . $\sigma(\cdot)$ is the activation function. By expanding Eq. (1), it can be observed that for a K -layer GNN model, computing the final output embedding h_v^K for node v involves its K -hop neighbors.

Graph sampling for GNN training. GNN training is usually conducted in mini-batches with each mini-batch computing the output embeddings for some seed nodes (i.e., the nodes whose labels are known) and updating the model according to a loss function that measures the difference between model output and ground-truth. Training is said to finish an epoch when all seed nodes are used once, and typically many epochs are required for the model to converge. As a seed node can have many K -hop neighbors, graph sampling is widely used to reduce training cost by sampling some of the neighbors for computation [23–28]. For instance, the popular node-wise sampling [23] uses a fan-out vector to specify the number of neighbors to sample and conducts neighbor sampling independently for the nodes in the same layer. For instance, the left plot of Figure 1 uses a fanout of $\langle 2, 2 \rangle$, which means that sampling is conducted for 2 steps, and each node samples 2 neighbors for both steps. In the first step, $\{v_3, v_5\}$ are sampled as the neighbors of the seed node v_0 ; in the second step, v_3 samples its neighbors $\{v_2, v_7\}$ while v_5 samples $\{v_9, v_{11}\}$.

3 OFFLINE SAMPLING

Challenge for out-of-core training. For graph datasets, the node features are usually (much) larger than the graph topology, and thus out-of-core training needs to store (most of) the node features on disk. For each mini-batch, the related node features need to be fetched from the disk to GPU memory to conduct model computation. For instance, in Figure 1, handling seed node v_0 requires the node features of $\{v_0, v_3, v_5, v_2, v_7, v_9, v_{11}\}$. However, disk is accessed with page size as minimum granularity (usually 4KB), and each node feature is usually much smaller than disk page size (e.g., the 128-dimension float vector of the Ogbn-papers100M dataset takes 512 bytes). As the required node features are not contiguous on disk, many small random reads are used, which cause read amplification and make the disk traffic for feature reading much larger than the required features (i.e., see Ginex in Table 1), yielding low I/O efficiency. For instance, in the right plot of Figure 1, we assume that two node features take up a disk page; training only needs to read 7 node features but the total disk traffic is 12 node features.

Offline sampling for data layout optimization. Each mini-batch of GNN training involves two main steps, i.e., *graph sampling* to determine the computation graph and the node features to use, and *model computation* to compute output embeddings for the seed nodes and update the model according to the loss function. Existing systems for GNN training couple the two steps of a mini-batch, i.e., they run the mini-batches sequentially, and each mini-batch first conducts graph sampling and then model computation. The insight of offline sampling is that we do not have to perform model computation immediately after finishing graph sampling for a mini-batch; instead, we can sample many mini-batches before model computation. By decoupling graph sampling and model computation, offline sampling collects the features to be accessed beforehand, which enables the following opportunities to optimize the data layout for efficient access during model computation.

- *Cache configuration to reduce disk access.* With the node features to be accessed by all mini-batches, we can rank the nodes by their access frequencies and cache more popular nodes in faster memory (e.g., GPU memory and CPU memory) to reduce disk access. Such a cache configuration is also optimal in that it minimizes the total number of node features fetched from the disk.
- *Feature packing to avoid read amplification.* For each mini-batch, we can first collect all node features it requires and store them contiguous as a large disk block (i.e., feature packing). During model computation, we can read all these features as a single disk block without read amplification.
- *Batched packing for many mini-batches.* If we conduct feature packing individually for each mini-batch, it will be inefficient because small random disk read is still needed to collect the required node features. However, when handling a large number of mini-batches, most of the node features are accessed by at least one of these mini-batches. This observation allows us to switch the feature packing scheme from *mini-batch oriented* to *feature partition oriented*. In particular, we can read a large partition of node features from disk each time, find the features in the partition that are required by each mini-batch, and append these

features to the disk storage of each mini-batch. This multi-batch packing is efficient as it involves only large sequential disk access.

Our DiskGNN exploits all the above optimization opportunities enabled by offline sampling with system designs. We note that feature packing essentially trades *disk space* for *access efficiency* because a node feature may be required by multiple mini-batches and thus replicated multiple times by packing. The increased disk space consumption is usually not a problem because disk capacity is cheap. When the space overhead of packing is too large, offline sampling may use *node reordering* [29, 30], a classical technique in graph processing, to reduce read amplification. The rationale is to renumber the graph nodes such that the node features accessed concurrently by the mini-batches are likely to be in the same disk page. Besides, offline sampling can store the graph samples and packed node features, which may be reused multiple times to save sampling and packing costs. It has been shown that reusing graph samples does not harm model accuracy [31].

In addition to disk-based training, offline sampling may also benefit cloud-based training by allowing *flexible instance selection*. This is because public clouds (e.g., AWS [32] and Azure [33]) provide machine instances with different configurations (e.g., memory capacity, CPU power, with or without GPU) and thus different prices; and with graph sampling decoupled from model computation, we can choose a proper instance for each of them to reduce the monetary cost. In particular, graph sampling requires the graph topology and conducts small random access, and thus it suits an instance with enough CPU memory to hold the graph topology. We do not need to hold the node features in CPU memory and may not use GPU because the computation of sampling is lightweight. Model computation involves neural networks and thus suits an instance with GPU. We can reduce the idle time of expensive GPU by conducting graph sampling and packing the node features beforehand on a cheaper instance.

4 DISKGNN SYSTEM OVERVIEW

Figure 2 depicts the overall architecture and workflow of DiskGNN. At initialization, DiskGNN takes the graph samples for many mini-batches and all node features of the graph as input and assumes that they are stored on the disk. The graph samples can be easily obtained by conducting graph sampling using existing GNN frameworks like DGL [22] and PyG [34]. Then, DiskGNN conducts pre-processing to construct a data layout for efficient access during model training. This is achieved by storing the node features in a *four-level feature store*, which is aimed to fully utilize the memory hierarchy and will be introduced shortly. After pre-processing, DiskGNN runs model training by going over the mini-batches to update the model. For each mini-batch, DiskGNN loads its graph sample from the disk and assembles the required node features from the *four-level feature store*, and the GPU uses these data to conduct model computation. The data reading and model computation of different mini-batches are overlapped with a training pipeline.

Note that DiskGNN can conduct pre-processing and training on different machines for low monetary cost because pre-processing does not require GPU. In this case, pre-processing determines the node features to be stored in GPU and CPU memory and writes

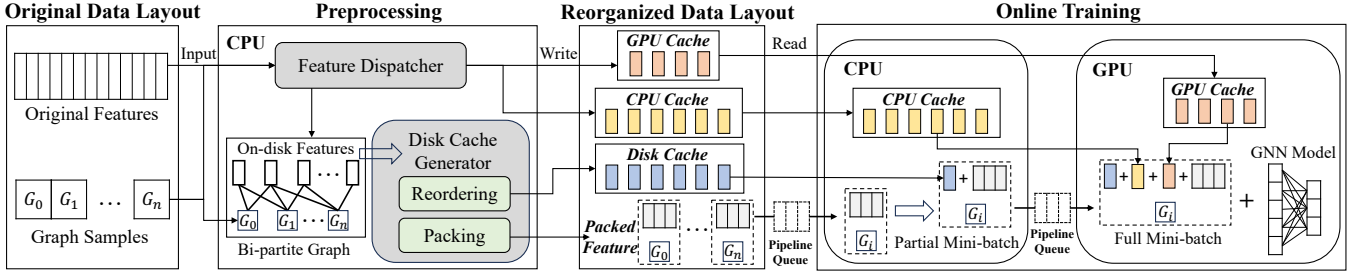


Figure 2: DiskGNN system architecture and workflow.

them as separate blocks on disk; the training machine loads the two feature blocks to initialize its GPU and CPU cache.

Four-level hierarchical feature store. During pre-processing, DiskGNN first goes over all graph samples to collect the access frequencies of all node features. We say nodes that are accessed more times are more popular. Then, DiskGNN determines where to store each node feature according to its popularity as follows:

- *GPU cache* stores the most popular node features, and accesses to these node features enjoy the high bandwidth of GPU memory. The GPU cache size is configured by excluding the working memory for model training from the total GPU memory.
- *CPU cache* stores the second popular node features, and the GPU accesses the CPU cache as unified virtual memory (UVM) [35] via PCIe. This usually does not cause read amplification because the access granularity of UVM is 50 bytes, which is typically smaller than a node feature. The CPU cache size is configured by reserving the memory to assemble the graph samples and node features of several mini-batches to prepare for training.
- *Disk cache* stores the third popular node features. As discussed in § 3, packing all node features for each mini-batch may consume large disk space because a node feature can be stored multiple times. DiskGNN allows the user to specify the maximum disk space the system can use and disk cache is activated when packing exceeds the space limit. The node features in the disk cache are not replicated, instead, they are processed by node reordering in the hope that the node features required by each mini-batch are stored in a small number of disk pages. As such, the disk cache reduces rather than eliminates read amplification.
- *Packed feature chunk* stores the node features that are not in the above three cache components. For each mini-batch, DiskGNN creates a disk chunk to store its packed features, and the graph sample of the mini-batch is also packed in the chunk as the node features and graph samples will be fetched together. Accesses to the packed feature chunks do not have read amplification because each chunk is usually larger than disk page size.

Instead of activating the disk cache after observing that packing uses too much space, DiskGNN decides whether and how to use the disk cache by analyzing the access frequencies of the node features. The details of determining the node features to store in the disk cache and node reordering are discussed in § 5.1, and how to conduct the pre-processing and fill in the four-level feature store efficiently is introduced in § 5.2.

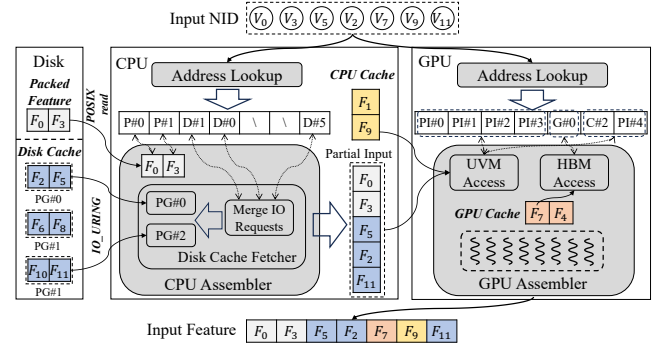


Figure 3: An example of feature assembling in DiskGNN. G#, C#, D#, P#, and Pl# denote that a feature locates in the GPU cache, CPU cache, disk cache, packed chunk, and partial input, respectively. PG refers to disk pages in the disk cache.

Feature assembling. During training, DiskGNN takes two steps to assemble the node features in the feature store for each min-batch. In the first step, the CPU reads the features in the disk cache and packed feature chunks and prepares them as *partial input* for the GPU. In the second step, the GPU reads the GPU cache, CPU cache, and partial input to obtain all the required features. DiskGNN uses HashMaps as address lookup tables in both steps to get knowledge of the requested feature locations. These tables translate the node IDs to feature addresses in the four-level feature store. Figure 3 provides a working example of the feature assembling process, where the required node features are {0, 3, 5, 2, 7, 9, 11}, and nodes {1, 9} and {7, 4} are stored in the CPU and GPU cache, respectively.

During CPU assembling, DiskGNN interprets the node IDs to address their locations on disk and launches disk I/O to read their features from the packed chunks (P#) and disk cache (D#). For the packed features, feature chunk {0, 3} is loaded via one disk page. For features {2, 5, 11} located in the disk cache, DiskGNN first merges the requests pointing to the same disk page to eliminate duplicate accesses and then reads the required pages. In particular, {2, 5} are in the same disk page due to node ordering and thus fetched via one page. For GPU assembling, DiskGNN interprets the node IDs to address their locations in CPU and GPU, including partial input (Pl#), CPU cache (C#) and GPU cache (G#). To collect all input features, DiskGNN launches UVM accesses to load the features for Pl# and C# and directly fetches features in GPU cache for G#.

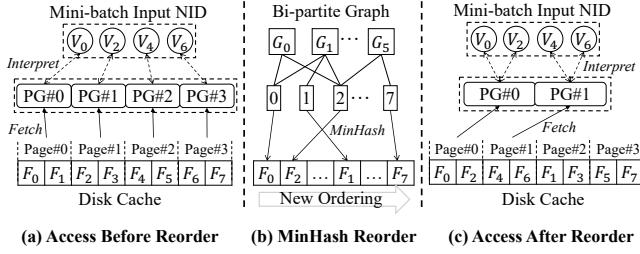


Figure 4: Feature access pattern before and after reordering. Minhash bucketing is used to reorder features in disk cache.

Algorithm 1 Disk Cache Reordering using MinHash

Input: A set of n graph samples $\{G_1, \dots, G_n\}$, disk cache entries $V_d = \{V_{d1}, \dots, V_{dm}\}$, number of hash functions k
Output: Reordered cached entries V_r

- 1: $H \leftarrow \emptyset$
- 2: $S \leftarrow [inf \text{ for range } |V_d|]$
- 3: *generate k hash functions*
- 4: **for** $i \leftarrow 1, \dots, k$ **do**
- 5: $H \leftarrow H \cup \{ \text{PERMUTE}(1, \dots, n) \}$
- 6: *iterate over the mini-batches*
- 7: **for** $i \leftarrow 1, \dots, n$ **do**
- 8: $(V_i, E_i) \leftarrow G_i, V_{in} \leftarrow V_i \cap V_d$
- 9: **for** $v \in V_{in}$ **do**
- 10: **for** $H_j \in H$ **do** // calculate minhash values
- 11: $S(v) \leftarrow \text{MIN}(S(v), H_j(i))$
- 12: $V_r \leftarrow V_d[\text{ARGSORT}(S)]$
- 13: **Return** V_r

5 SYSTEM DESIGNS

In this section, we discuss the major design components and optimizations of DiskGNN in detail. First, we describe how to organize disk cache to trade off between read amplification and storage overhead in §5.1. Then, we discuss optimizations to speed up feature packing for pre-processing in §5.2, followed by the pipelined training of DiskGNN in §5.3.

5.1 Segmented Disk Cache

The goal of using a disk cache shared among all graph samples is to reduce the high storage overhead caused by the duplication of the packed node features for different graph samples. However, this would bring about random disk accesses and read amplification when fetching features from disk cache. A promising solution to alleviate read amplification is to promote better data locality via smart node reordering. By storing node features in the disk cache according to a better node ordering, I/O requests to separate disk pages can potentially be merged into the same page. In this way, random feature read will access fewer disk pages and thus reduce the I/O traffic. In this part, we first discuss how DiskGNN reorders nodes on a global disk cache and analyze the limitations. Then, we introduce the proposed method to achieve a better trade off between disk space consumption and read amplification.

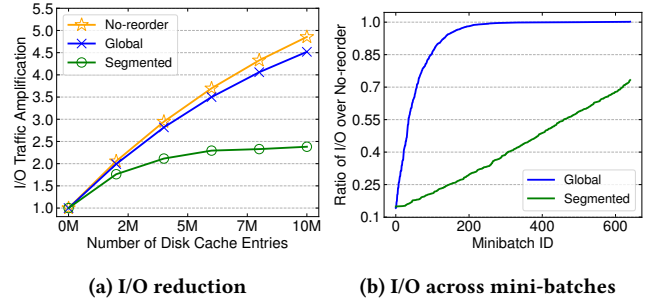


Figure 5: Effect of node reordering of global and segmented disk cache on Friendster dataset. (a) shows I/O amplification for an epoch and (b) shows the ratio of I/O over non-reordered disk cache for different mini-batches.

Reordering for global disk cache. Figure 4 shows how DiskGNN conducts node reordering to achieve better data locality on disk. Before reordering, the required features for nodes $\{0, 2, 4, 6\}$ reside in four different disk pages and four random reads are needed to load them. Suppose the underlying disk page can accommodate 2 node features. Then the four random reads will incur 2x read amplification. To find a better node ordering, DiskGNN models the nodes whose features are in the disk cache and all the graph samples using a bi-partite graph in which a node is connected to a graph sample if it appears in the graph sample. With this bi-partite graph, the graph reordering method HashOrder [29] can be used to group nodes that have the most similar neighbors (i.e., required by similar sets of graph samples) and store them contiguously on disk. Since each node is required by a set of graph samples, thus we adopt a hashing method like MinHash to discover set similarities. More complex graph reordering techniques like Gorder [30] are not used since they are much more expensive than HashOrder which provides comparable reordering quality.

Algorithm 1 shows how to generate a MinHash value for each node and use it for reordering. Specifically, given n total graph samples, we randomly generate a permutation for $1, \dots, n$ which will be used to calculate the hash signature for a graph sample. For every graph sample, we incrementally update the min-wise hash value for each of the graph sample’s nodes assigned to the disk cache using the hash signature of the graph sample (line 11). After iterating over all the graph samples, we obtain the MinHash value for each disk cache node. By sorting nodes according to their hash values, nodes that are required by the same set of graph samples are grouped in adjacent locations. In practice, multiple hash functions can be used to reduce the probability of hash collision, and empirically using 2 hash functions provides good reordering quality. By reordering, requests to node feature 0 and 2 are located in the same page (so do 4 and 6) and can be merged into one single disk access. Therefore, only two random reads are needed for node features $\{0, 2\}$ and $\{4, 6\}$, which cuts down I/O by 50%.

Unfortunately, reordering nodes for a global disk cache shared by all graph samples has little impact on reducing read amplification. Figure 5a shows the result of global reordering on the Friendster

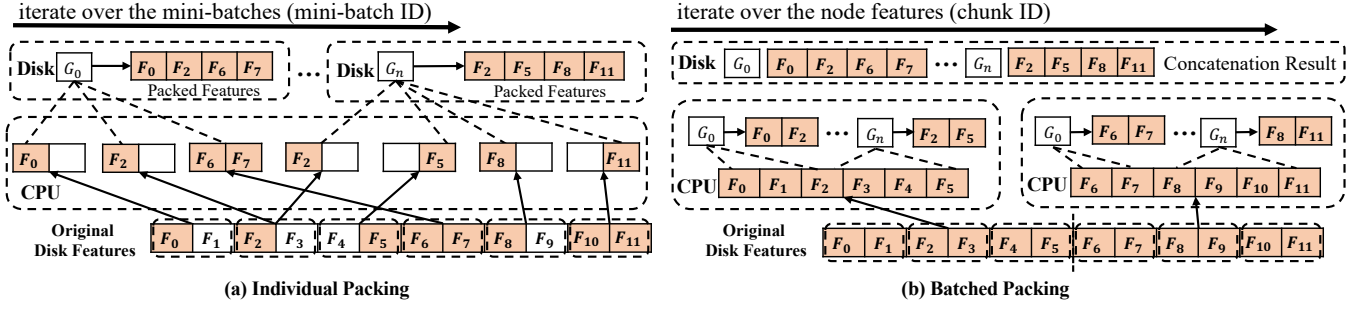


Figure 6: Optimization of feature packing during DiskGNN's pre-processing.

Algorithm 2 Search Method for Segmented Disk Cache

Input: Graph samples $G = \{G_1, \dots, G_n\}$, total nodes V , CPU cache V_c , GPU cache V_g , disk space constraint c , feature dimension f
Output: Number of disk cache entries m , segment size s

- 1: $\text{count} \leftarrow [0 \text{ for range } |V|]$
- 2: **for** $G_i = (V_i, E_i) \in G$ **do**
- 3: $V_{cm} \leftarrow V_i - V_c - V_g$
- 4: **for** $v \in V_{cm}$ **do**
- 5: $\text{count}[v] \leftarrow \text{count}[v] + 1$
- 6: $V_d, V_p \leftarrow V[\text{count} > 1], V[\text{count} = 1]$
- 7: $\text{disk_space} \leftarrow ((|V_d| + |V_p|) \times |G|/i) \times f \times 4$
- 8: **if** $\text{disk_space} \leq c$ **do**
- 9: **Return** $m \leftarrow |V_d|, s \leftarrow i$

dataset. The I/O traffic grows with more node entries stored in the disk cache due to more random disk access with read amplification. It is observed that reordering can only reduce total I/O traffic by less than 10% in one epoch with varying disk cache sizes. We further examine the ratio of I/O traffic over non-reordered baseline for every mini-batch in Figure 5b. We can see that only about one-third of the mini-batches (i.e., graph samples) have noticeable I/O reduction from this global reordering, and only one-tenth of the mini-batches achieve more than 50% I/O reduction. This is reasonable as the GPU and CPU cache already store node features with high access frequencies while the remaining nodes are shared more uniformly among graph samples, so a single global order is unlikely to achieve good data locality for all graph samples.

Local reordering for segmented disk cache. The observation that a small percentage of graph samples benefit from reordering in one global disk cache motivates us to divide the graph samples into multiple segments and create a locally-reordered disk cache for each segment. Specifically, given a segment size, we use the same metric (i.e., node access frequency) to extract disk cache entries for the graph samples and perform node reordering as introduced before in Algorithm 1 on this disk cache. During training, each graph sample fetches its required features from the shared disk cache of its corresponding segment (as well as its packed feature chunk store). Figure 5b shows that, with a locally-reordered disk cache per 50 graph samples, the I/O traffic is significantly reduced, compared with using a global reordered disk cache.

Approximate search method. To materialize the segmented disk cache, we need to determine the number of disk cache entries m and segment size s . As is discussed above, putting more features in disk cache brings about more random disk reads, and enlarging the segment size degrades the reordering quality (measured by I/O traffic). On the other hand, setting a very small disk cache and segment size results in many replicated packed features across graph samples, consuming too much disk space. To this end, we need to search for the sweet point of m and s , which achieves low read amplification while satisfying the user's disk space constraint.

The brutal-force solution is to iterate over all possible combinations of m and s that satisfy the disk space constraint, calculate the I/O traffic for an epoch, and select the configuration with the lowest I/O traffic. However, as a 2-dimensional grid search, the brutal-force method needs to generate and reorder the segmented disk cache repeatedly for every combination of m and s , which is too costly. To solve this issue, we propose an approximate method to find the near-optimal parameters using only 1-dimensional search on the s .

Algorithm 2 describes the approximate search process. We assume that the storage consumption is similar for different s when m is small since most of the on-disk features are assigned to the packed feature chunks rather than disk cache. Also, the I/O traffic will be lower for smaller s with the same m , as good data locality is more likely to remain with smaller groups. Based on the above observations, we can simply set m to the number of nodes with accessed counts > 1 (i.e., at least accessed by two different graph samples) and simplify the problem to a 1-dimensional linear search on the segment size. This is equivalent to storing all node features in the disk cache since node features with accessed count $= 1$ will always be grouped together, in the same manner as packed features. Furthermore, we use the storage consumption and I/O traffic of a segment to estimate the total results of an epoch, by using a scaling factor. This enables us to read each graph sample from disk only once with the growth of the segment size. The search terminates when the estimated disk consumption satisfies the constraint. Experimental results in §7 show that the proposed approximate method can speed up the search time at a significant scale while providing near-optimal configurations for m and s .

5.2 Batched Feature Packing

During the pre-processing stage of DiskGNN, we need to fetch node features from their original on-disk layout and write them back to contiguous disk space as packed feature chunks. However, this involves random reads to on-disk features, incurring high I/O cost due to read amplification and thus long pre-processing overhead. Next, we first present a naive design that extracts and packs features for one mini-batch at a time. We then discuss how DiskGNN turns random reads to sequential reads with batched feature packing.

Individual packing. The naive method processes each mini-batch independently, as shown in Figure 6a. Specifically, it does random reads to fetch a mini-batch’s required node features from the disk at each iteration. It faces two performance issues. First, each random read is small as it only fetches a single node’s feature, resulting in I/O amplification. Second, for nodes that appear in multiple mini-batches, their features are read from the disk multiple times, resulting in redundant I/O. Consequently, the individual packing approach has poor I/O efficiency. As shown in Figure 14, it brings an extra 31% overhead for training an epoch with DiskGNN when amortizing the pre-processing time to every epoch.

Batched packing. To eliminate I/O amplification and duplicate reads, we switch to performing packing for one feature partition at a time instead of one mini-batch at a time. We call the resulting solution, batched packing method, because it simultaneously packs features for all mini-batches. Specifically, we split the node features of the entire graph into a few logical partitions so that each of which fit into the CPU memory. At each iteration, we load a partition of consecutive node features from disk, perform feature packing for all graph samples within this partition in memory, and write back the partial output to disk.

Figure 6b gives an example of batched packing. At the first iteration, the feature partition containing node {0–5} is loaded using a single sequential read of three underlying SSD pages with no read amplification. Nodes within the loaded feature partition are needed by different graph samples. For instance, graph sample G_0 requires nodes {0, 2} and G_n requires nodes {2, 5} from the feature partition {0–5}. We write the required node contiguously in memory for each graph sample. The dispatch of node features to different graph samples can be fully parallelized without any need for synchronization. After gathering the required node features for the current partition, we perform a sequential write for each graph sample to append its partial feature chunk to the graph’s packed feature file on disk. Once all the feature partitions have been processed, each graph’s packed feature file is complete on disk. In practice, because each graph sample can typically gather more features than that fit in a 4KB disk page, the sequential writes are large, thereby avoiding write amplification and improving I/O efficiency.

Batch packing effectively addresses the two major drawbacks of individual packing by replacing small random reads with large sequential reads, and ensuring that each node feature is loaded only once throughout the process. We point out that the batched packing method can also be parallelized across machines to gain further speedup, as there are no data dependencies during packing across different feature partitions. However, this is out of the scope of this project and we leave it to future work.

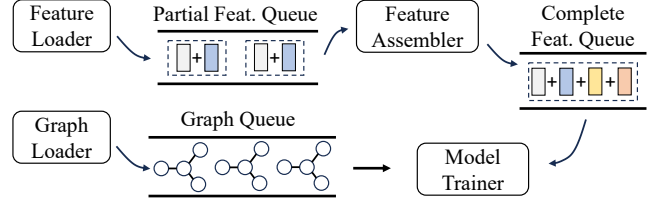


Figure 7: DiskGNN’s training pipeline.

5.3 Pipelined Training

Naive execution that trains each mini-batch by first fetching its constituent node features from disk results in low CPU and GPU utilization during I/O access. Like other out-of-core training systems [20, 36], we leverage a pipelined design to overlap the computation and I/O access of adjacent mini-batches. The key difference from existing systems [20, 36] is that DiskGNN uses more fine-grained pipeline stages to handle the loading and assembly of node features from our four-level feature store.

The pipelined procedure is presented in Figure 7. DiskGNN divides the work required to train a mini-batch into four pipeline stages, each of which is handled by a worker thread. Workers adhere to the producer-consumer pattern using shared queues to execute the different stages of consecutive mini-batches in parallel. The four pipeline stages consist of: ① feature loading ② feature assembling ③ graph loading ④ model training.

We note that four pipeline stages are non-linear with two separate dependency paths: ① → ② → ④ and ③ → ④. On the first pipeline path, *feature loader* starts by fetching the on-disk features into consecutive CPU memory from disk cache and packed feature chunks. The fetched features form a partial set of a mini-batch’s node features and are put into the queue for the next pipeline stage. Then the worker, *feature assembler*, assembles features from both the CPU and GPU memory to form a mini-batch’s full set of node features in one CUDA kernel. To do so, it performs direct memory accesses to the GPU cache and UVA access to the CPU cache as well as the mini-batch’s fetched partial features in the CPU memory. After assembling, the complete features of a mini-batch are sent to the complete-feature-queue. On the second pipeline path, *graph loader* fetches the graph topology of each mini-batch from disk to the graph-queue in CPU memory. As the last stage for both pipeline paths, *model trainer* retrieves both the graph sample and the complete features of a mini-batch from the two corresponding queues, and conducts GNN training computation for this mini-batch. By using the same ordering to process mini-batches in both pipeline paths, DiskGNN guarantees that heads of both the complete-feature-queue and the graph-queue belong to the same mini-batch. As the GNN model and graph samples are typically small and can not saturate the GPU, we put *model trainer* and *feature assembler* on separate CUDA streams to improve GPU utilization.

With pipelining, the four worker threads can run tasks concurrently to work on different mini-batches. For example, when *model trainer* is performing GNN computation on mini-batch n , *graph loader* can fetch the graph sample for mini-batch $n+1$, *feature assembler* can assemble the complete features for mini-batch $n+1$, and *feature loader* can load the on-disk features for mini-batch $n+2$. This

allows for the overlap of SSD reads, CPU to GPU data transfer, and GPU computation so that the overall performance is bottlenecked by the longest stage as opposed to the sum of all stages.

6 IMPLEMENTATION

DiskGNN is developed using the C++ library of Pytorch [37] as the backend. We utilize DGL [22], a popular open-source framework for graph learning, to store graph samples in disk and perform model training. The implementation considerations consist of three parts:

- I/O operations: DiskGNN uses `pread`[38] for sequential disk access to fetch packed feature chunks, which can fully saturate the SSD bandwidth with a single thread. For random disk accesses to fetch features in disk cache, DiskGNN leverages `io_uring` [39] and uses 4 threads with each thread holding a ring to launch I/O requests, which is observed to have nearly-saturated I/O performance. OpenMP[40] is used to execute that 4 threads and subsequent `memcpy` operations in parallel. For all I/O operations, we use `POSIX open` [41] as the file descriptor with `O_Direct` flag to bypass the OS page cache and directly access the SSD.
- Feature assembling: For feature assembling in GPU, DiskGNN uses Unified Virtual Addressing (UVA) [35] in GPU kernels to fetch features resident on CPU main memory. For the address lookup operations both in CPU and GPU to generate corresponding feature locations, we prepare the interpreted address locations during pre-processing and directly load them from disk during online training. This saves the interpreting cost in the training pipeline and avoids duplicated address generation for each graph sample across epochs.
- Training pipeline: For the producer-consumer-based pipelining of DiskGNN, each shared queue is set to have a size limit of 2, which can fully overlap the stages while not causing too much extra memory occupation.

Easy-to-use API. DiskGNN has API that offers users an exceptionally simple interface, enabling them to build efficient data layout and conduct training based on their disk size budget with just a single line of Python code.

```
def DiskGNN_train(dataset_path : PATH, disk_size : int, cpu_size :
    ↳ int, gpu_size : int, kwargs)
```

DiskGNN initially arranges the data layout for the CPU and GPU cache using `cpu_size` and `gpu_size`, respectively. Then, a lightweight search algorithm is employed to identify the data layout for segmented disk cache under the constraint of `disk_size`. Subsequently, batched packing is used to efficiently pack on-disk features. After completing all data orchestration, training can start by integrating the I/O engine, feature assembler, and model trainer.

7 EVALUATION

In this part, we conduct extensive experiments to evaluate DiskGNN and compare them with state-of-the-art disk-based GNN training systems. The main observations are that:

- *DiskGNN consistently yields shorter training time than the baselines while matching the best model accuracy of them.*
- *DiskGNN performs well across different configurations.*
- *The designs of DiskGNN, e.g., node reordering, batched packing, and training pipeline, are effective in improving efficiency.*

Table 2: Graph datasets used in the experiments.

Attributes	Friendster	Papers	MAG240M	IGB260M
Abbr.	FS	PS	MG	IG
Vertex count	66M	111M	244M	269M
Edge count	3.6B	3.3B	3.4B	3.9B
Graph size (GB)	28.5	25.9	27.9	30.8
Feature size (GB)	31.3	52.9	117	129
Train nodes (%)	N/A	1.09	0.45	5.06

Table 3: Model accuracy (%) comparison for the systems.

Systems		Datasets		
		Papers100M	MAG240M	IGB-HOM
SAGE	Ginex	65.85	67.90	58.96
	DiskGNN	65.91	67.79	59.03
	MariusGNN	64.01	65.50	58.77
GAT	Ginex	65.03	66.48	56.43
	DiskGNN	65.03	66.53	56.69
	MariusGNN	OOM	OOM	OOM

7.1 Experiment Settings

Datasets and models. We use the four graph datasets in Table 2 for experiments and refer to them by abbreviations subsequently. These datasets are publicly available and widely used to evaluate GNN models and systems. Since FS and IG are undirected graphs, we replace each undirected edges with two directed edges. For PS, we add a reverse edge for each directed edge to enlarge the receptive field of each node during neighbor aggregation. As FS only provides the graph topology (i.e., without node features and labels), we randomly generate a 128-dimension float vector for each node as the feature and select 1% of its nodes as the seed nodes for training by assigning fake labels.

We choose two representative models, i.e., GraphSAGE [23] and GAT [42], and adopt their popular hyper-parameter settings. In particular, GraphSAGE uses the mean aggregation function while GAT uses multi-head attention for neighbor aggregation. The hidden embedding dimension of GraphSAGE is 256 while a hidden embedding dimension of 32 and 4 attention heads are used for GAT. Following the open-source example from DGL [43], both GraphSAGE and GAT are set to have 3 layers. For graph sampling, we use node-wise neighbor sampling with a fanout of [10,15,20], and the number of seed nodes (i.e., batch size) in a mini-batch is 1024.

Baseline systems. We compare DiskGNN with two state-of-the-art disk-based GNN training systems, i.e., Ginex [18] and MariusGNN [20]. As introduced in § 1, Ginex accesses each node feature individually and manages the nodes cached in CPU memory using the Belady’s algorithm; MariusGNN organizes the graph into edge chunks and node partitions and samples only the memory-resident node features for training. We do not compare with Helios [21] and GIDS [19] because Helios is not open-sourced, and GIDS uses GPU-initiated disk I/O, which is only supported by the latest GPUs. They both adopt the fine-grained feature access of Ginex and thus also suffer from the read amplification problem. As a naive baseline,

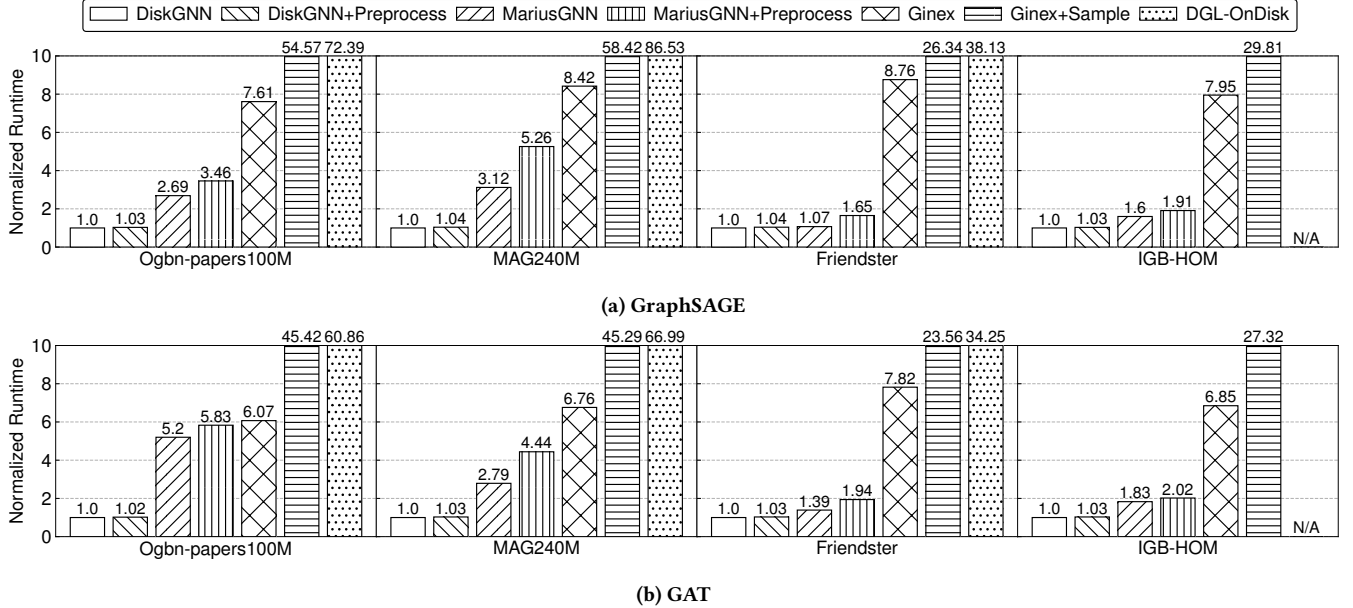


Figure 8: Normalized epoch time for training the two GNN models, the epoch time of DiskGNN is set as 1.0 in each case.

we also altered DGL for disk-based training (called DGL-OnDisk) by directly using pread to read the node features from disk.

Platform and metrics. We conduct the experiments on a AWS g5.48xlarge [44] instance with a 96-core AMD EPYC 7R32 CPU, 748GB RAM, 2×3.8 TB NVMe SSD, and an NVIDIA A10G GPU with 24GB memory. To simulate the case of large graphs that exceed CPU memory, we set memory constraints for the systems as different proportions of the graph features, with 10% by default. The NVMe SSD of the machine provides 2.5GBps bandwidth and 625,000 IOPS at the maximum. The GPU is connected to the host CPU via PCIe 3.0 with a full bandwidth of 7GBps. The operating system is Ubuntu 20.04, and the software is CUDA 11.7 [45], Python 3.9.18 [46], PyTorch 2.0.1 [47], DGL 1.1.2 [43], and PyG 2.5.0 [48].

We compare the systems in terms of both model accuracy and training efficiency. For model accuracy, we report the test accuracy at the epoch when the highest validation accuracy is achieved for each system. For PS and MG, we run 50 epochs of training to reach convergence. For IG, only 20 epochs are needed as it has more seed nodes. We do not use FS in accuracy evaluation because it does not provide node features and labels. For training efficiency, we run each system for 5 epochs and record the average time of the latter 4 epochs, leaving the first epoch for warming up. The default CPU memory is set as 10% of the graph feature size to simulate the case of large graphs that exceed CPU memory. We also adjust the memory constraint to check its influence on the epoch time.

7.2 Main Results

Model accuracy. Table 3 reports the model accuracy achieved by the systems. For PS and IG, the accuracy is measured on the test set, while MG uses the validation set as it only provides labels for the validation set. The results show that DiskGNN matches

the model accuracy of Ginex for both GraphSAGE and GAT, and the small differences may be caused by random factors such as parameter initialization and random graph sampling. However, the model accuracy of MariusGNN is noticeably lower than Ginex and DiskGNN. For instance, for the PS graph and GraphSAGE model, the accuracy degradation of MariusGNN is 2.4%, which is large for GNN models and may be unacceptable for applications such as recommendation. For GAT, MariusGNN runs out-of-memory (OOM) when evaluating the model accuracy for all datasets.

Epoch time. Figure 8 reports the epoch time of the systems. In each case (i.e., model plus dataset), we normalize the results by treating the epoch time of DiskGNN as 1 because the epoch time spans a large range for different datasets, which will make the figure difficult to read if we use real epoch time. Note that the results of DiskGNN, Ginex, and Marius do not include their pre-processing time. To understand the influence of pre-processing, we also report DiskGNN + preprocess, Marius + preprocess, and Ginex + sample, which amortize the pre-processing time of the systems over the training epochs. During pre-processing, Ginex conducts disk-based graph sampling while Marius organizes the graph into edge chunks and node partitions. DGL-OnDisk can not finish an epoch in 10 hours on IG, and thus we report N/A for it.

Figure 8 shows that DiskGNN consistently outperforms all baseline systems across the four datasets and two GNN models. In particular, the speedup of DiskGNN over Ginex is over 6x in all cases and can be 8.76x at the maximum. This is because Ginex suffers from severe read amplification by reading each node feature individually from disk while DiskGNN enjoys efficient disk access due to its data layout optimizations. Compared with MariusGNN, DiskGNN has about 2x speedup in 6 out of the 8 cases, while providing superior model accuracy. The speedup on FS is smaller because the node access for FS is more uniform with the popular nodes being less

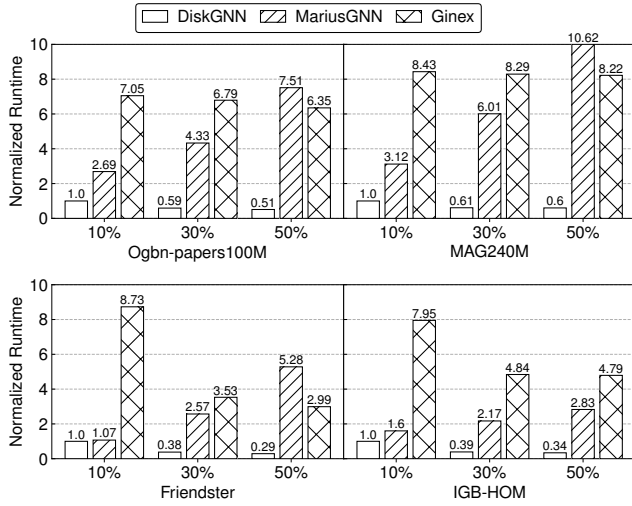


Figure 9: Normalized epoch time with different CPU memory constraints for training the GraphSAGE model.

dominant, which makes the CPU and GPU cache less effective. Regarding DGL-OnDisk, the speedup of DiskGNN is significant (i.e., 86.53x at the maximum) because DGL-OnDisk needs to read every node feature from disk (without CPU and GPU cache), suggesting that a naive solution is inefficient. Considering the pre-processing time, the difference between DiskGNN + preprocess and DiskGNN is within 5% for all cases, indicating the pre-processing of DiskGNN is efficient. The pre-processing of MariusGNN also does not add too much overhead but Ginex has a long pre-processing time because disk-based graph sampling is slow.

Memory constraint. Figure 9 compares the epoch time of DiskGNN, MariusGNN, and Ginex for training the GraphSAGE model. We adjust the cache memory the systems can use as percentages (i.e., 10%, 30% and 50%) of the node feature size of the datasets. The results show that DiskGNN trains consistently faster than MariusGNN and Ginex with different memory constraints, achieving a maximum speedup of 10.62x and 8.73x, respectively. DiskGNN observes a diminishing return in training efficiency when enlarging the cache memory, i.e., increasing from 30% to 50% feature size brings a much smaller speedup than from 10% to 30% feature size. This is because most accesses to node features are served by the GPU and CPU caches with a reasonable memory size, and thus further increasing the memory is not very effective in reducing disk access.

MariusGNN has longer epoch time at larger memory size because it loads more edge chunks and node partitions from disk to fill in the CPU memory. Moreover, graph sampling for the on-CPU partitions will involve more neighbors, leading to longer sampling time and model training time as the graph samples involve more edges. We note that loading more partitions enables MariusGNN to achieve higher model accuracy but its accuracy is still lower than Ginex and DiskGNN. For instance, with the memory being 50% of the feature size, MariusGNN improves the model accuracy by 0.71% (from 64.01% to 64.72%) on the PS graph but the degradation from Ginex and DiskGNN (i.e., 65.85% and 65.91%) is still significant.

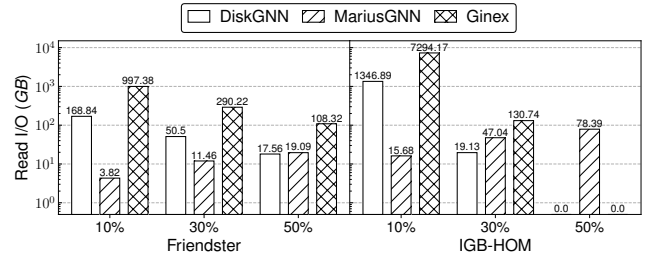


Figure 10: Disk traffic adjusting the CPU memory constraints.

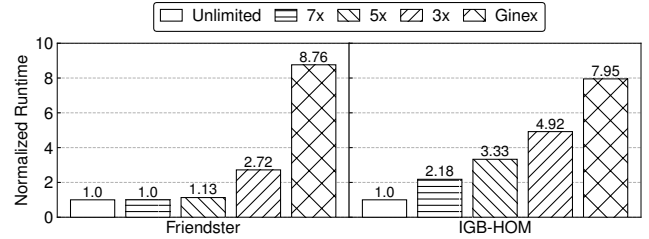


Figure 11: Normalized epoch time with different disk space constraints for training the GraphSAGE model.

Disk traffic. To understand the results in Figure 9, Figure 10 report the average amount of data the systems read from disk in an epoch. We include only FS and IG due to the page limit (similarly for some other experiments). Note that the disk traffic results are the same for GraphSAGE and GAT. The results show that the disk traffic of DiskGNN is never above 1/5 of Ginex under all cache configurations and datasets, which explains the speedup of DiskGNN over Ginex. When the memory size is 50% of the node features, DiskGNN and Ginex almost have no disk traffic to read the node features on the IG graph, justifying the diminishing return of increasing CPU memory. As we have explained, MariusGNN has larger disk traffic with larger CPU memory because it loads more node partitions and edge chunks to fill in the CPU memory.

Disk space constraint. Figure 11 reports the epoch time of DiskGNN with different constraints on the disk space DiskGNN uses, which is specified as the times (i.e., 7x, 5x and 3x) of the feature size. We include Ginex as a reference, and the results of PS and MG are omitted because they use less disk space than the original feature size even if we only use packing. When disk space is unlimited, FS uses 5.39x of the feature size while IG uses 10.19x of the feature size. This explains why FS observes a very small change in epoch time when switching from unlimited to 5x feature size. The results show that DiskGNN has a longer training time when using smaller disk space. This is because DiskGNN needs to store more node features in the disk cache instead of packed feature chunks, and the disk cache relies on node reordering to reduce read amplification while packed feature chunks eliminate read amplification.

Disk consumption. The maximum disk space DiskGNN can use is affected by the cache memory size because when the GPU and

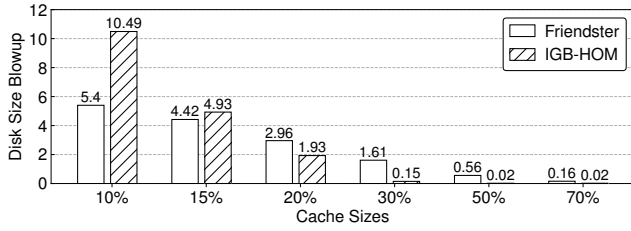


Figure 12: Disk space usage under different CPU cache sizes.

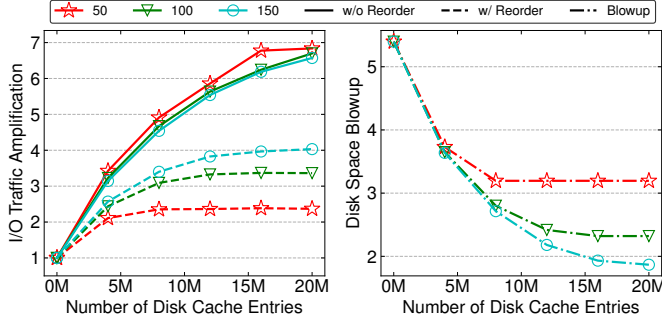


Figure 13: Effectiveness of segmented disk cache on the FS graph. Left is the disk traffic amplification for feature reading, right is the disk space usage w.r.t. the original features.

CPU cache hold more node features, fewer node features need to be stored in the packed feature chunks on disk. Figure 12 reports how the maximum disk space usage changes when adjusting the cache memory size, and both disk space and cache memory are relative to the size of the node features. The results show that the disk space usage reduces quickly when increasing the cache memory size. Specifically, we observe that only about 20% memory cache ratio is needed to keep the disk space consumption below 2 times of the original features. The reduction of the disk space usage is more significant on the IG graph because its node accesses are more skewed towards the popular nodes and thus the node feature cache is more effective in reducing disk access.

7.3 Micro Experiments

Segmented disk cache with reordering. In Figure 13, we evaluate the effectiveness of the segmented disk cache and node reordering on the FS graph. We use three configurations (i.e., 50, 100, and 150) for the number of min-batches in a segment (i.e., segment size). The results of the other graphs are similar and omitted due to the space limit. The left plot of Figure 13 suggests that our MinHash-based node reordering is effective in reducing the disk traffic across different segment sizes. Moreover, the disk traffic reduction of reordering is larger with a smaller segment size (e.g., 50 vs 150). This is because the feature reordering suits the min-batches better when considering a small number of mini-batches. The right plot shows that using a smaller segment size constantly yields a larger disk space consumption. Moreover, the disk consumption has a lower bound for a specific segment size and the minimum value is achieved by storing

Table 4: Efficiency and quality of the approximate method to search for disk cache configuration compared with the brutal-force search. *Blowup* is the disk space to use, *I/O Amp.* is disk traffic amplification, and *Time* is the search time.

Blowup		Methods				Speedup
		Brutal Force		Approximate		
		I/O Amp.	Time (s)	I/O Amp.	Time (s)	
FS	3x	2.98x	257.0	2.58x	0.99	259.60x
	5x	1.33x	75.00	1.09x	0.18	416.67x
IG	3x	5.10x	6288	4.85x	22.8	275.83x
	5x	4.11x	4755	3.39x	9.76	487.27x
	7x	3.01x	3261	2.28x	4.61	707.52x

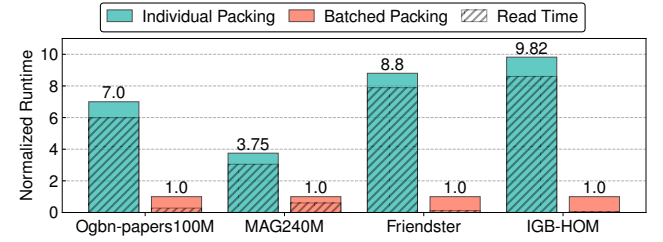


Figure 14: Running time of naive individual packing and our optimization batched packing for pre-processing.

all node features in the disk cache. At this point, the disk space consumption is the multiple segments of disk cache themselves, which is smaller with a larger segment size. We also observe that different segment sizes produce similar disk consumption when the size of the disk cache is small, which validates the assumption of our approximate search method for the configuration of disk cache size and segment size.

Approximate search method. Table 4 compares the search time and result quality of our approximate method to search for the configuration of disk cache in § 5.1 with the brute-force search that returns the optimal configuration. The resulting quality can be measured by the disk traffic amplification, and lower amplification means high quality. Brute-force search may have lower result quality than our method because it needs a step size when iterating over the segment size, as generating the disk cache and reordering repeatedly for every segment size is too costly, and this prevents brute-force search from finding the optimal configuration. Specifically, we set the step size for FS and IG as 100 and 1000 respectively, which is roughly 1/10 of the total number of mini-batches. The results show that our approximate method reduces the search time of brute-force by over 250x while yielding comparing or even better result quality, mainly by eliminating repeated graph loading, disk cache generation, and local reordering. Moreover, the disk consumption curve in Figure 13 also verifies the assumption that disk consumption is almost the same under small disk cache sizes, making it reasonable for us to do the approximation.

Batched packing. Figure 14 shows the speedup of batched packing over individual packing across 4 datasets. For both solutions, we

Table 5: Pipelined training vs. sequential execution.

	CPU cache size	Methods		Speedup
		Sequential	Pipeline	
FS	10%	165.3	96.67	1.71x
	30%	88.98	36.51	2.44x
	50%	54.24	28.12	1.93x
IG	10%	1901.82	960.73	1.98x
	30%	652.35	312.71	2.09x
	50%	641.26	324.61	1.98x

mark the read time during end-to-end preprocessing in the figure. With individual packing, read time is consistently the bottleneck, constituting between 81% and 90% of the total preprocessing time. Batched packing addresses this bottleneck by replacing duplicated random reads of on-disk features with sequential reads without duplication. As shown in Figure 14, batched packing achieves an average 7.34x speedup in total preprocessing time, especially with an average 61x speedup for feature loading. The speedup on FS and IG is generally larger since they need to load more features under a more uniform access skewness and a low cache hit ratio. With the significant optimization of batched packing, the overhead of preprocessing becomes negligible for the entire training pipeline.

GNN training pipelining. Table 5 validates the effectiveness of the producer-consumer-based GNN training pipeline. Sequential execution refers to the implementation that uses only a single thread to conduct graph loading, feature loading, feature assembling, and model training, and pipelined execution conducts them in parallel. Results show that the proposed stage division and pipelining gives a maximal speedup of 2.44x and an average speedup of over 2x compared with sequential execution. Under a small cache size ratio (e.g., 10%), the training pipeline is bottlenecked by heavy disk feature loading, whereas graph loading or model computation becomes the dominant part when the cache size ratio is high (e.g., 50%).

8 RELATED WORK

Graph learning frameworks. DGL [22] and PyG [34] are two popular deep learning frameworks on graphs, which provide comprehensive user interfaces to express various GNN algorithms and efficient CPU and GPU operators for graph sampling and model training. We enjoy these optimizations by building DiskGNN upon them. On top of these two frameworks, there are many systems focusing on GPU kernel optimizations during GNN training, such as GNNAdvisor [49], Graphiler [50], TC-GNN [51]. These optimizations are orthogonal to DiskGNN. Furthermore, they all assume the graph topology and node features can fit in CPU main memory and do not optimize the data loading from disk to CPU when graph data is large enough, which is the main focus of DiskGNN.

Large-scale GNN training systems. To handle large-scale graphs that can not fit in CPU main memory, many systems utilize multiple machines to train the GNN model in parallel with each machine holding a partition of graph data in CPU. NeuGraph [52], ROC [53], PipeGCN [54], BNS-GCN [55] and DGCL [56] are representative early distributed GNN systems but adopt full-graph training which

brings about high GPU memory consumption for intermediate hidden embeddings and easily exceeds the GPU capacity when scaling up. Recent systems adopt a sampling-based approach to control the number of neighbors for aggregation [15–17, 57–60]. Though they can scale up GNN training, all these systems need a cluster to hold the graph data, which is expensive in practice for huge industrial graphs with tens of billions of nodes and edges. Also, they suffer from heavy communication costs between machines to exchange node features and intermediate embeddings.

Our-of-core DNN workload. There are also systems developed for training large-scale DNN workloads on disk. FlexGen [61] aggregates storage resources from the GPU, CPU, and disk, enabling 175B parameter model inference on a single GPU. Dragon [62] and FlashNeuron [63] employ GPU-direct storage access to retrieve intermediate data from NVMe SSD while minimizing interference with applications running on the CPU. The techniques introduced in these systems can not directly be applied to GNN training as they all focus on the GPU capacity limit due to the huge amount of parameters in DNN. While for training GNN models, which are much smaller, the CPU memory is typically the concern as it can not hold the entire input node features. Moreover, the data access patterns in DNN training are different from those in GNN training.

9 CONCLUSION

We present DiskGNN, an efficient framework designed to support large-scale GNN training, specifically tailored for scenarios where the graph features exceed CPU memory capacity and require offloading to disk. DiskGNN incorporates offline sampling with feature packing to bridge the I/O efficiency and model accuracy in one system, and adopts a four-layer hierarchical feature store to reduce disk access. Several optimizations are proposed and integrated in DiskGNN, including reordering on the segmented disk cache to reduce I/O traffic with better data locality, batched packing to alleviate the preprocessing overhead by transforming duplicated random disk reads into sequential disk reads without duplication, and pipeline training to overlap disk access with other operations. Extensive experiments demonstrate that DiskGNN significantly outperforms existing GNN training systems, showing an average speedup of 8x over baseline systems.

REFERENCES

- [1] Jizhe Wang, Pipei Huang, Huan Zhao, Zhibo Zhang, Binqiang Zhao, and Dik Lun Lee. Billion-scale commodity embedding for e-commerce recommendation in alibaba. In *Proceedings of the 24th ACM SIGKDD International Conference on Knowledge Discovery and Data Mining*, page 839–848, 2018.
- [2] Mark Weber, Giacomo Domeniconi, Jie Chen, Daniel Karl I. Weidele, Claudio Bellei, Tom Robinson, and Charles E. Leiserson. Anti-money laundering in bitcoin: Experimenting with graph convolutional networks for financial forensics. *CoRR*, abs/1908.02591, 2019.
- [3] Fuli Feng, Xiangnan He, Xiang Wang, Cheng Luo, Yiqun Liu, and Tat-Seng Chua. Temporal relational ranking for stock prediction. *ACM Trans. Inf. Syst.*, 37(2):27:1–27:30, 2019.
- [4] Sungmin Rhee, Seokjun Seo, and Sun Kim. Hybrid approach of relation network and localized graph convolutional filtering for breast cancer subtype classification. In *Proceedings of the Twenty-Seventh International Joint Conference on Artificial Intelligence, IJCAI-18*, pages 3527–3534, 2018.
- [5] Laura Garton, Caroline Haythornthwaite, and Barry Wellman. Studying online social networks. *J. Comput. Mediat. Commun.*, 3(1):0, 1997.
- [6] Thomas N. Kipf and Max Welling. Semi-supervised classification with graph convolutional networks. In *5th International Conference on Learning Representations, ICLR*, 2017.

- [7] Muhan Zhang and Yixin Chen. Link prediction based on graph neural networks. In Samy Bengio, Hanna M. Wallach, Hugo Larochelle, Kristen Grauman, Nicolò Cesa-Bianchi, and Roman Garnett, editors, *Advances in Neural Information Processing Systems 31: Annual Conference on Neural Information Processing Systems, NeurIPS*, pages 5171–5181, 2018.
- [8] Anton Tsitsulin, John Palowitch, Bryan Perozzi, and Emmanuel Müller. Graph clustering with graph neural networks. *CoRR*, abs/2006.16904, 2020.
- [9] Shiwen Wu, Fei Sun, Wentao Zhang, Xu Xie, and Bin Cui. Graph neural networks in recommender systems: A survey. *ACM Comput. Surv.*, 55(5), 2022.
- [10] Daixin Wang, Yuan Qi, Jianbin Lin, Peng Cui, Quanhui Jia, Zhen Wang, Yanming Fang, Quan Yu, Jun Zhou, and Shuang Yang. A semi-supervised graph attentive network for financial fraud detection. In *2019 IEEE International Conference on Data Mining, ICDM*, pages 598–607, 2019.
- [11] Kehang Han, Balaji Lakshminarayanan, and Jeremiah Liu. Reliable graph neural networks for drug discovery under distributional shift, 2021.
- [12] Weihua Hu, Matthias Fey, Marinka Zitnik, Yuxiao Dong, Hongyu Ren, Bowen Liu, Michele Catasta, and Jure Leskovec. Open graph benchmark: Datasets for machine learning on graphs. *arXiv preprint arXiv:2005.00687*, 2020.
- [13] Arpandeep Khatua, Vikram Sharma Maitlthody, Bhagyashree Taleka, Tengfei Ma, Xiang Song, and Wen-mei Hwu. Igb: Addressing the gaps in labeling, features, heterogeneity, and size of public graph datasets for deep learning research. In *Proceedings of the 29th ACM SIGKDD Conference on Knowledge Discovery and Data Mining*, 2023.
- [14] SNAP. Stanford large Network Dataset Collection. <https://snap.stanford.edu/data/index.html>, 2023. [Online; accessed September-2023].
- [15] Da Zheng, Chao Ma, Minjie Wang, Jinjing Zhou, Qidong Su, Xiang Song, Quan Gan, Zheng Zhang, and George Karypis. Distdgl: Distributed graph neural network training for billion-scale graphs, 2021.
- [16] Zhenkun Cai, Qihui Zhou, Xiao Yan, Da Zheng, Xiang Song, Chenguang Zheng, James Cheng, and George Karypis. Dsp: Efficient gnn training with multiple gpus. In *Proceedings of the 28th ACM SIGPLAN Annual Symposium on Principles and Practice of Parallel Programming*, page 392–404, 2023.
- [17] Swapnil Gandhi and Anand Padmanabha Iyer. P3: Distributed deep graph learning at scale. In *15th USENIX Symposium on Operating Systems Design and Implementation (OSDI 21)*, pages 551–568, 2021.
- [18] Yeonhong Park, Sunhong Min, and Jae W. Lee. Ginex: Ssd-enabled billion-scale graph neural network training on a single machine via provably optimal in-memory caching. *Proc. VLDB Endow.*, 15(11):2626–2639, 2022.
- [19] Jeongmin Brian Park, Vikram Sharma Maitlthody, Zaid Qureshi, and Wen mei Hwu. Accelerating sampling and aggregation operations in gnn frameworks with gpu initiated direct storage accesses, 2024.
- [20] Roger Waleffe, Jason Mohoney, Theodoros Rekatsinas, and Shivaram Venkataraman. Mariusgcn: Resource-efficient out-of-core training of graph neural networks. In *Proceedings of the Eighteenth European Conference on Computer Systems*, pages 144–161, 2023.
- [21] Jie Sun, Mo Sun, Zheng Zhang, Jun Xie, Zuocheng Shi, Zihan Yang, Jie Zhang, Fei Wu, and Zeke Wang. Helios: An efficient out-of-core gnn training system on terabyte-scale graphs with in-memory performance. *arXiv preprint arXiv:2310.00837*, 2023.
- [22] Minjie Wang, Lingfan Yu, Da Zheng, Quan Gan, Yu Gai, Zihao Ye, Mufei Li, Jinjing Zhou, Qi Huang, Chao Ma, Ziyue Huang, Qipeng Guo, Hao Zhang, Haibin Lin, Junbo Zhao, Jinyang Li, Alexander J Smola, and Zheng Zhang. Deep Graph Library: Towards Efficient and Scalable Deep Learning on Graphs. In *Proceedings of the ICLR Workshop on Representation Learning on Graphs and Manifolds*, 2019.
- [23] William L. Hamilton, Zitao Ying, and Jure Leskovec. Inductive representation learning on large graphs. In Isabelle Guyon, Ulrike von Luxburg, Samy Bengio, Hanna M. Wallach, Rob Fergus, S. V. N. Vishwanathan, and Roman Garnett, editors, *Advances in Neural Information Processing Systems 30: Annual Conference on Neural Information Processing Systems, NeurIPS*, pages 1024–1034, 2017.
- [24] Difan Zou, Ziniu Hu, Yewen Wang, Song Jiang, Yizhou Sun, and Quanquan Gu. Layer-dependent importance sampling for training deep and large graph convolutional networks. In *Advances in Neural Information Processing Systems 32: Annual Conference on Neural Information Processing Systems, NeurIPS*, pages 11247–11256, 2019.
- [25] Wenbing Huang, Tong Zhang, Yu Rong, and Junzhou Huang. Adaptive sampling towards fast graph representation learning. In *Proceedings of the 32nd International Conference on Neural Information Processing Systems, NeurIPS’18*, page 4563–4572, 2018.
- [26] Jianfei Chen, Jun Zhu, and Le Song. Stochastic training of graph convolutional networks with variance reduction. In *Proceedings of the 35th International Conference on Machine Learning, ICML 2018, Stockholm, Sweden, July 10–15, 2018*, volume 80, pages 941–949, 2018.
- [27] Minji Yoon, Théophile Gervet, Baoxu Shi, Sufeng Niu, Qi He, and Jaewon Yang. Performance-adaptive sampling strategy towards fast and accurate graph neural networks. In *The 27th ACM SIGKDD Conference on Knowledge Discovery and Data Mining*, pages 2046–2056, 2021.
- [28] Hanqing Zeng, Hongkuan Zhou, Ajitesh Srivastava, Rajgopal Kannan, and Viktor K. Prasanna. Accurate, efficient and scalable graph embedding. In *IEEE International Parallel and Distributed Processing Symposium, IPDPS*, pages 462–471, 2019.
- [29] Tianyi Zhang, Aditya Desai, Gaurav Gupta, and Anshumali Shrivastava. Hashorder: Accelerating graph processing through hashing-based reordering, 2024.
- [30] Hao Wei, Jeffrey Xu Yu, Can Lu, and Xuemin Lin. Speedup graph processing by graph ordering. In *Proceedings of the 2016 International Conference on Management of Data*, page 1813–1828, 2016.
- [31] Haitian Jiang, Renjie Liu, Xiao Yan, Zhenkun Cai, Minjie Wang, and David Wipf. Musegcn: Interpretable and convergent graph neural network layers at scale. *arXiv preprint arXiv:2310.12457*, 2023.
- [32] AWS. <https://aws.amazon.com/>, 2024. [Online; accessed April-2024].
- [33] Azure. <https://azure.microsoft.com>, 2024. [Online; accessed April-2024].
- [34] Matthias Fey and Jan Eric Lenssen. Fast graph representation learning with pytorch geometric. *CoRR*, abs/1903.02428, 2019.
- [35] NVIDIA Corporation. Unified Addressing. https://docs.nvidia.com/cuda/cuda-driver-api/group__CUDA__UNIFIED.html, 2024. accessed, April-2024.
- [36] Jason Mohoney, Roger Waleffe, Henry Xu, Theodoros Rekatsinas, and Shivaram Venkataraman. Marius: Learning massive graph embeddings on a single machine. In *15th USENIX Symposium on Operating Systems Design and Implementation (OSDI)*, 2021.
- [37] Adam Paszke, Sam Gross, Francisco Massa, Adam Lerer, James Bradbury, Gregory Chanan, Trevor Killeen, Zeming Lin, Natalia Gimelshein, Luca Antiga, et al. Pytorch: An imperative style, high-performance deep learning library. *Advances in neural information processing systems*, 32, 2019.
- [38] Linux. POSIX pread. <https://man7.org/linux/man-pages/man2/pwrite.2.html>, 2024. accessed, April-2024.
- [39] Linux. io_uring. https://man7.org/linux/man-pages/man7/io_uring.7.html, 2024. accessed, April-2024.
- [40] OpenMP. OpenMP. <https://www.openmp.org>, 2024. accessed, April-2024.
- [41] Linux. POSIX open. <https://man7.org/linux/man-pages/man2/open.2.html>, 2024. accessed, April-2024.
- [42] Petar Veličković, Guillem Cucurull, Arantxa Casanova, Adriana Romero, Pietro Liò, and Yoshua Bengio. Graph Attention Networks. In *International Conference on Learning Representations (ICLR)*, 2018.
- [43] DGL. Deep Graph library. <https://www.dgl.ai>, 2024. [Online; accessed April-2024].
- [44] AWS. Amazon EC2 G5 instance. <https://aws.amazon.com/cn/ec2/instance-types/g5>, 2024. [Online; accessed April-2024].
- [45] NVIDIA. CUDA Toolkit. <https://developer.nvidia.com/cuda-toolkit>, 2024. [Online; accessed April-2024].
- [46] Python. Python. <https://www.python.org/downloads/release/python-398/>, 2024. [Online; accessed April-2024].
- [47] PyTorch. PyTorch. <https://pytorch.org>, 2024. [Online; accessed April-2024].
- [48] PyG. PyTorch Geometric. <https://www.pyg.org>, 2024. [Online; accessed April-2024].
- [49] Yuke Wang, Boyuan Feng, Gushu Li, Shuangchen Li, Lei Deng, Yuan Xie, and Yufei Ding. {GNNAdvisor}: An adaptive and efficient runtime system for {GNN} acceleration on {GPUs}. In *15th USENIX symposium on operating systems design and implementation (OSDI 21)*, pages 515–531, 2021.
- [50] Zhiqiang Xie, Minjie Wang, Zihao Ye, Zheng Zhang, and Rui Fan. Graphiler: Optimizing graph neural networks with message passing data flow graph. *Proceedings of Machine Learning and Systems*, 4:515–528, 2022.
- [51] Yuke Wang, Boyuan Feng, Zheng Wang, Guyue Huang, and Yufei Ding. Tc-gnn: Bridging sparse gnn computation and dense tensor cores on gpus. In *USENIX Annual Technical Conference (USENIX ATC)*, pages 149–164, 2023.
- [52] Lingxiao Ma, Zhi Yang, Youshan Miao, Jilong Xue, Ming Wu, Lidong Zhou, and Yafei Dai. NeuGraph: Parallel deep neural network computation on large graphs. In *Proceedings of the 2019 USENIX Annual Technical Conference (USENIX ATC)*, pages 443–458, 2019.
- [53] Zhihao Jia, Sina Lin, Mingyu Gao, Matei Zaharia, and Alex Aiken. Improving the accuracy, scalability, and performance of graph neural networks with ROC. In *Proceedings of the Machine Learning and Systems (MLSys)*, pages 187–198, 2020.
- [54] Cheng Wan, Youjie Li, Cameron R Wolfe, Anastasios Kyriklidis, Nam Sung Kim, and Yingyan Lin. Pipegcn: Efficient full-graph training of graph convolutional networks with pipelined feature communication. *arXiv preprint arXiv:2203.10428*, 2022.
- [55] Cheng Wan, Youjie Li, Ang Li, Nam Sung Kim, and Yingyan Lin. Bns-gcn: Efficient full-graph training of graph convolutional networks with partition-parallelism and random boundary node sampling. *Proceedings of Machine Learning and Systems*, 4:673–693, 2022.
- [56] Zhenkun Cai, Xiao Yan, Yidi Wu, Kaihao Ma, James Cheng, and Fan Yu. Dgcl: an efficient communication library for distributed gnn training. In *Proceedings of the Sixteenth European Conference on Computer Systems*, page 130–144, 2021.
- [57] Zeyuan Tan, Xiulong Yuan, Congjie He, Man-Kit Sit, Guo Li, Xiaozhe Liu, Baole Ai, Kai Zeng, Peter Pietzuch, and Luo Mai. Quiver: Supporting gpus for low-latency, high-throughput gnn serving with workload awareness, 2023.

- [58] Tianfeng Liu, Yangrui Chen, Dan Li, Chuan Wu, Yibo Zhu, Jun He, Yanghua Peng, Hongzheng Chen, Hongzhi Chen, and Chuanxiong Guo. {BGL}:{GPU-Efficient} {GNN} training by optimizing graph data {I/O} and preprocessing. In *20th USENIX Symposium on Networked Systems Design and Implementation (NSDI 23)*, pages 103–118, 2023.
- [59] Jianbang Yang, Dahai Tang, Xiaoni Song, Lei Wang, Qiang Yin, Rong Chen, Wenyuan Yu, and Jingren Zhou. Gnnlab: a factored system for sample-based gnn training over gpus. In *Proceedings of the Seventeenth European Conference on Computer Systems*, pages 417–434, 2022.
- [60] Jie Sun, Li Su, Zuocheng Shi, Wenting Shen, Zeke Wang, Lei Wang, Jie Zhang, Yong Li, Wenyuan Yu, Jingren Zhou, et al. Legion: Automatically pushing the envelope of {Multi-GPU} system for {Billion-Scale} {GNN} training. In *2023 USENIX Annual Technical Conference (USENIX ATC 23)*, pages 165–179, 2023.
- [61] Ying Sheng, Lianmin Zheng, Binhang Yuan, Zhuohan Li, Max Ryabinin, Beidi Chen, Percy Liang, Christopher Ré, Ion Stoica, and Ce Zhang. Flexgen: High-throughput generative inference of large language models with a single gpu. In *International Conference on Machine Learning*, pages 31094–31116. PMLR, 2023.
- [62] Pak Markthub, Mehmet E. Belviranli, Seyong Lee, Jeffrey S. Vetter, and Satoshi Matsuoka. Dragon: Breaking gpu memory capacity limits with direct nvm access. In *SC18: International Conference for High Performance Computing, Networking, Storage and Analysis*, pages 414–426, 2018.
- [63] Jonghyun Bae, Jongsung Lee, Yunho Jin, Sam Son, Shine Kim, Hakbeom Jang, Tae Jun Ham, and Jae W. Lee. FlashNeuron: SSD-Enabled Large-Batch training of very deep neural networks. In *19th USENIX Conference on File and Storage Technologies (FAST 21)*, pages 387–401, 2021.